Electronic Supplementary Material (ESI) for RSC Advances.

Supporting Information

Template-free Synthesis of 3D Hierarchical Amorphous Aluminum Oxide Microspheres with Broccoli-like Structure and their Application in Fluoride Removal

Dongjuan Kang, Shengrui Tong, Xiaolin Yu* and Maofa Ge*

Experimental Section

Synthesis of aluminum oxide microspheres

All of the reagents were analytically pure, and were purchased from Sinopharm Chemical Regent Beijing Co., Ltd. All of the reagents used are of analytical purity and used without further purification. Deionized water was used throughout the synthesis and treatment processes.

The synthesis of aluminum oxide microspheres was simply achieved by a solvothermal reaction followed by calcination in air. In a typical synthesis, Aluminium isopropoxide ($Al(OiPr)_3$) (6.127g, 30mmol) was injected into acetic acid (HAc), and then the solution was stirred for several minutes. The mixture was transferred to a Teflon-lined stainless steel autoclave and maintained at 200 °C for 2 h. After cooling to room temperature naturally, the precipitates were collected by centrifugation, thoroughly washed with deionized water and ethanol several times each, and dried in an oven at 60 °C for 12 h to get white powders of the precursor. Finally, the samples were calcined in a muffle furnace at 300 °C for 3 h in air, and then cooled down to room temperature naturally. For comparison, the commercially available Al_2O_3 was calcined at 300 °C for 3 h used as adsorbent for fluoride removal.

Materials characterization

The phase and composition of the as-prepared precursors and products were characterized by powder X-ray diffraction (XRD) using a Rigaku D/max 2500 diffractometer at a voltage of 40 kV and a current of 200 mA with Cu Kα radiation (λ=1.5406 Å), employing a scanning rate 0.02 °s^{-1} in the 2θ ranging from 3 to 80 °. The morphology of the obtained products was observed by Hitachi S-4800 scanning electron microscope (SEM) operating at 10 kV, the transmission electron microscope (TEM) and High-resolution transmission electron microscopy (HR-TEM) were performed on JEOL JEM-2011 at an acceleration voltage of 200 kV. Thermogravimetric analysis (TGA) measurement was performed from room temperature to 800 ^{o}C with a heating rate of 10 ^{o}C/min in air on a PE Pyris. The specific surface area was measured by nitrogen adsorption at 77 K (BET method) using an automated gas sorption analyzer (Quantachrome Instruments, autosorb-iQ). The pore size distribution is evaluated using the density functional theory (DFT) method. A Tensor 27 Fourier transform infrared spectroscopy (FTIR) was used to verify the presence of functional groups in the adsorbent. X-ray photoelectron spectroscopy (XPS) was performed on ESCALab220i-XL electron spectrometer from VG Scientific using 300W Al Kα radiation. ^{27}Al solid-state NMR spectra were obtained on BRUKER AVANCE III 400 spectrometer operating at 104.01 MHz equipped with a 4 mm rotor spun at 12 kHz. Isoelectric point (IEP) of the adsorbent was determined by the Zetasizer Nano zeta potentiometric analyser.

Adsorption experiments

Fluoride stock solutions were prepared by dissolving NaF into deionized water, respectively. The working solutions for all experiments were freshly prepared from the stock solution. All adsorption and regeneration experiments were carried out in a temperature controlled (at 25±1 °C) shaker using 150 mL shaking flasks containing fluoride solution with different initial concentrations for a predetermined contact time at 200 rpm. Adsorption isotherms were conducted with fluoride concentrations ranging from 5-150 mg/L, pH=7 and the adsorbent dose was kept as 0.5 g/L for all the experiments. Adsorption experiments were carried out in duplicate and the average data were used to evaluate the adsorption performance. Adsorption envelope was obtained in batch experiments by varying pH (pH 2-11). The fluoride concentration (50mg/L) and adsorbent dose (0.5g/L) were kept constant. The pH of each sample was adjusted by the addition of standard acid (0.1 mol/L HCl) and base solutions (0.1 mol/L NaOH). Samples were allowed to react for 12 h in a temperature controlled (at 25±1 °C) shaker using 150 mL shaking flasks. After equilibration, the pH of each sample was measured, and samples were subsequently filtered and analysed. Moreover, regeneration test was carried out under conditions of C_0=10 mg/L, adsorbent dose kept as 1 g/L and 1 mmol/L NaOH solution selected as a regenerant.

In our experiments, ion chromatography (ICS-900, Dionex) was used to analyze the concentration of fluoride, respectively. The adsorption capacity qe (mg/g) was calculated by the following equation:

$$q_e = \frac{(C_0 - C_e)V}{m} \tag{1}$$

where C_0 (mg/L) and C_e (mg/L) are the initial and equilibrium concentration of fluoride, respectively; V (L) is the solution volume and m (g) is the mass of the adsorbent.

The Langmuir adsorption model is used to calculate the maximum adsorption capacity, which can be expressed in the following form:

$$q_e = \frac{q_m b C_e}{1 + b C_e} \tag{2}$$

where C_e is the equilibrium concentration of the anions in solution (mg/L); q_e is the amount of anions adsorbed per unit mass of adsorbent at equilibrium (mg/g); q_m denotes the theoretical saturated adsorption capacity (mg/g); b is Langmuir constant related to the adsorption-desorption energy and to the affinity of binding sites for anions (L/mg).

The pseudo-second-order model has been widely used to describe the pollutants adsorption from aqueous solution. It can be expressed in the following form:

$$\frac{t}{q_t} = \frac{1}{k_2 q_e^2} + \frac{t}{q_\mathrm{e}} \tag{3}$$

where q_t and q_e are the adsorption capacity at time t and equilibrium, respectively; k_2 is pseudo-second-order rate constants. On the basis of the experimental data, the adsorption capacity of q_e, q_t and k_2 could be concluded from the slope and intercept respectively.

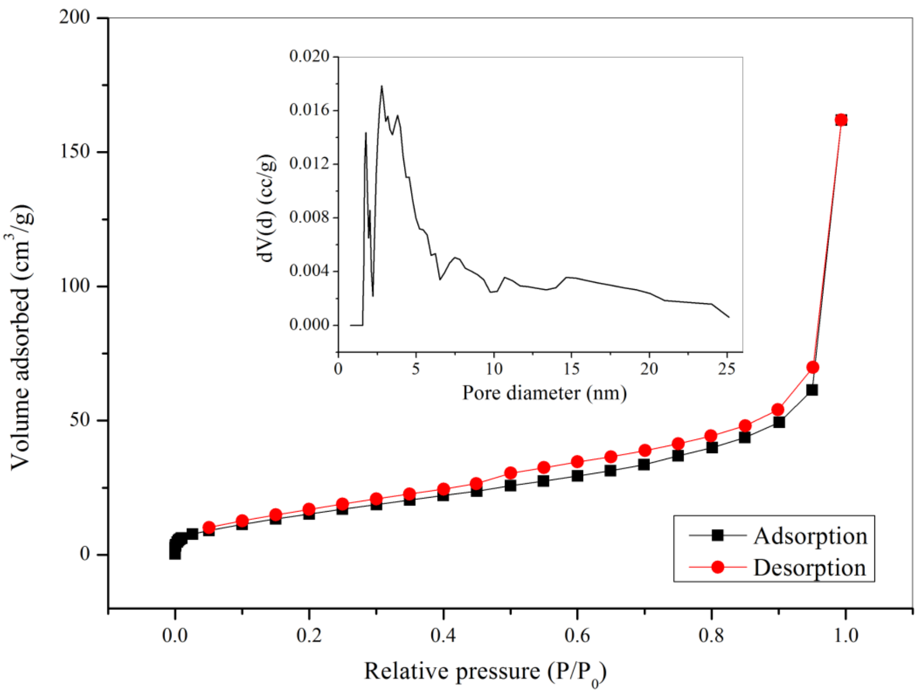

Fig. S1. N_2 adsorption-desorption isotherms for the precursor and (inset) the corresponding pore size distribution curve

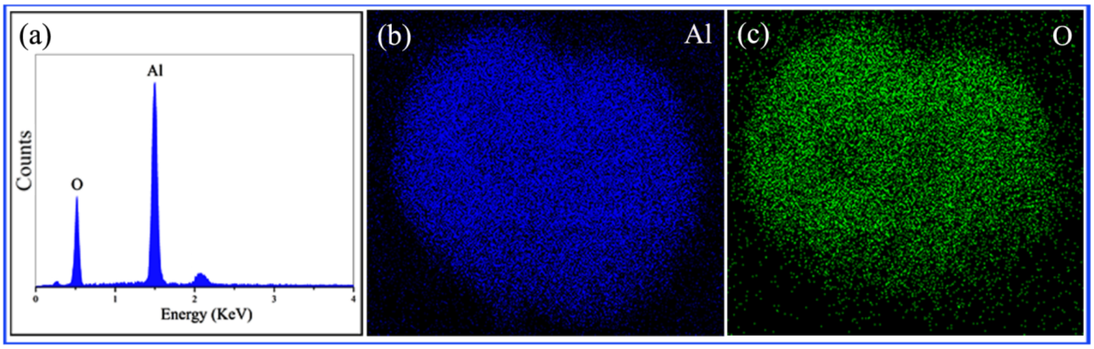

Fig. S2. (a) SEM-EDX and (b) elemental mapping spectra of the final product.

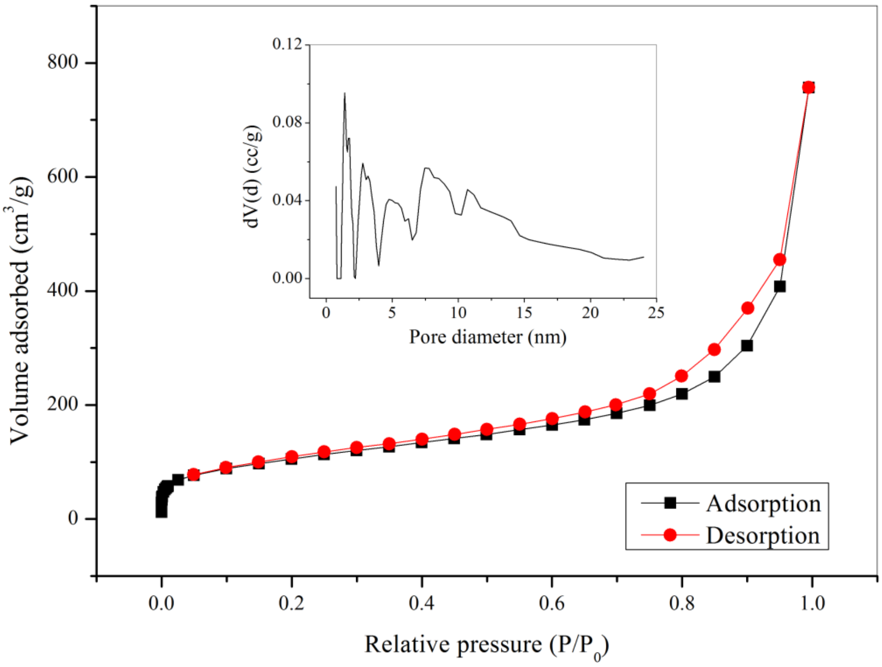

Fig. S3. N_2 adsorption-desorption isotherms for the final product and (inset) the corresponding pore size distribution curve.

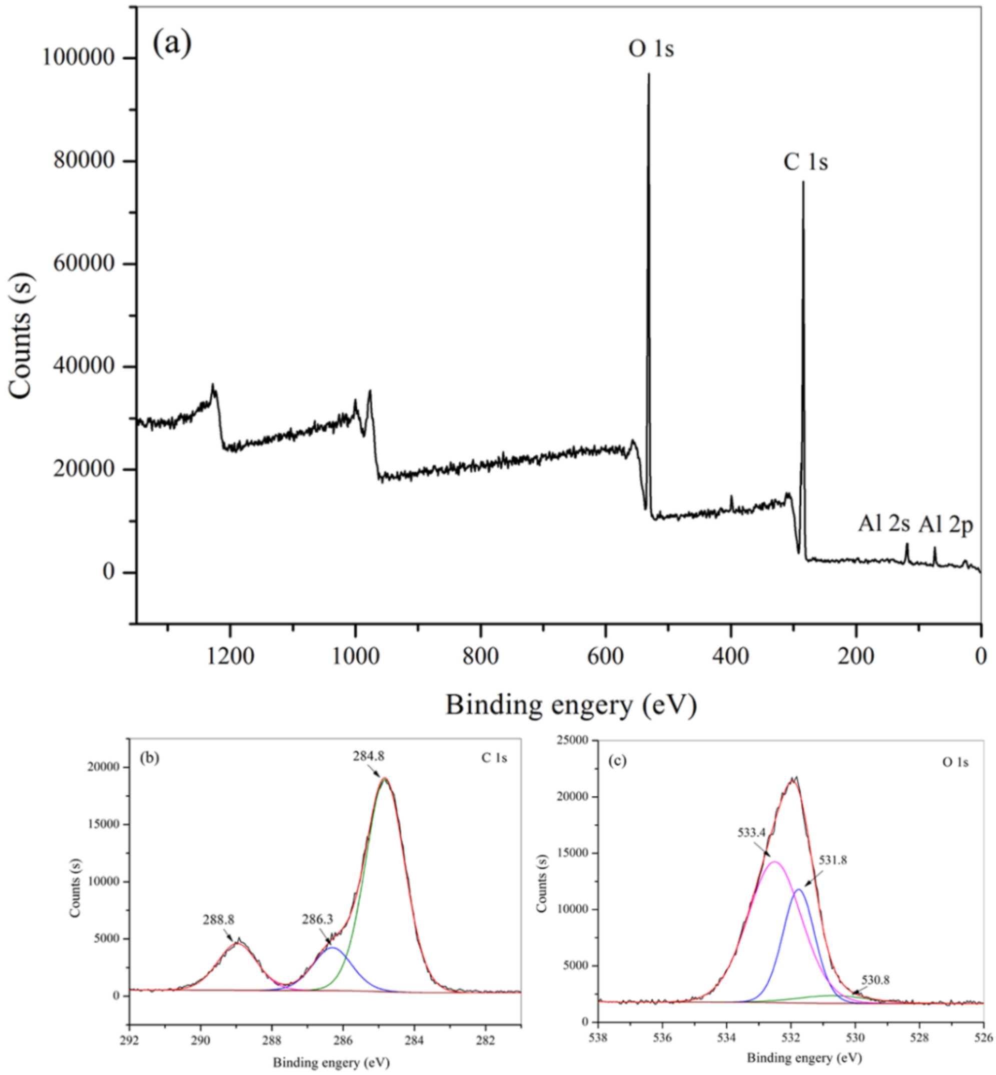

Fig. S4. XPS spectra of the final product; (a) full-range XPS spectrum; high-resolution XPS of (b) C1s and (c) O 1s

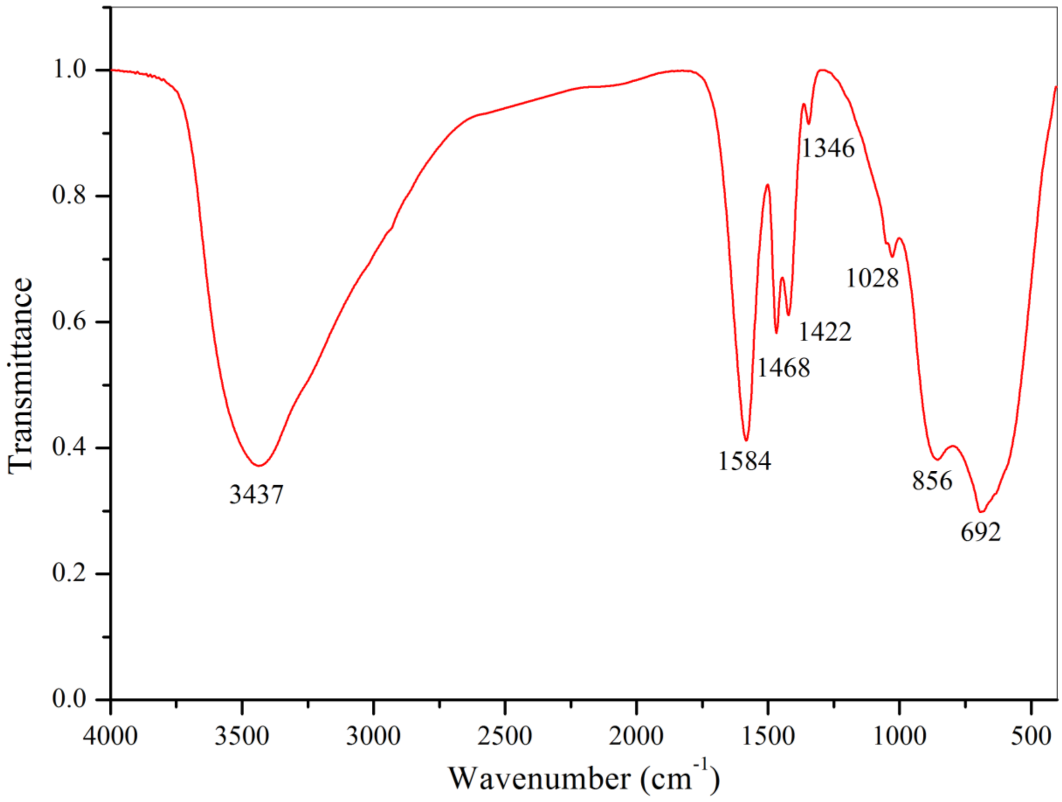

Fig. S5. FTIR spectrum of the final product

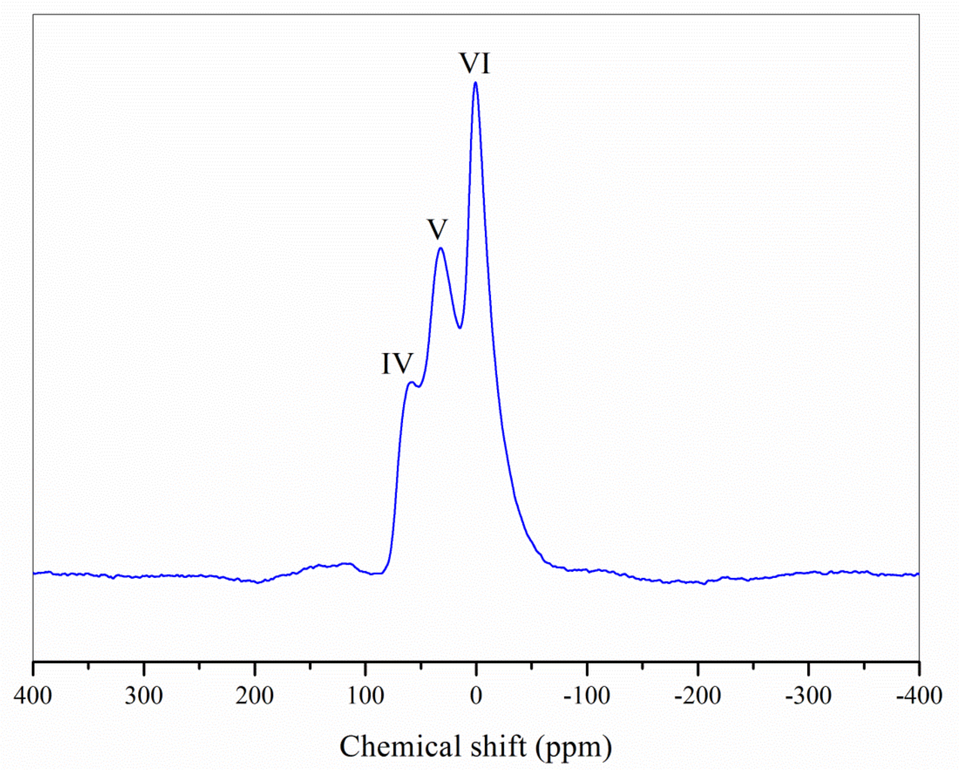

Fig. S6. ^{27}Al NMR spectrum of the final product.

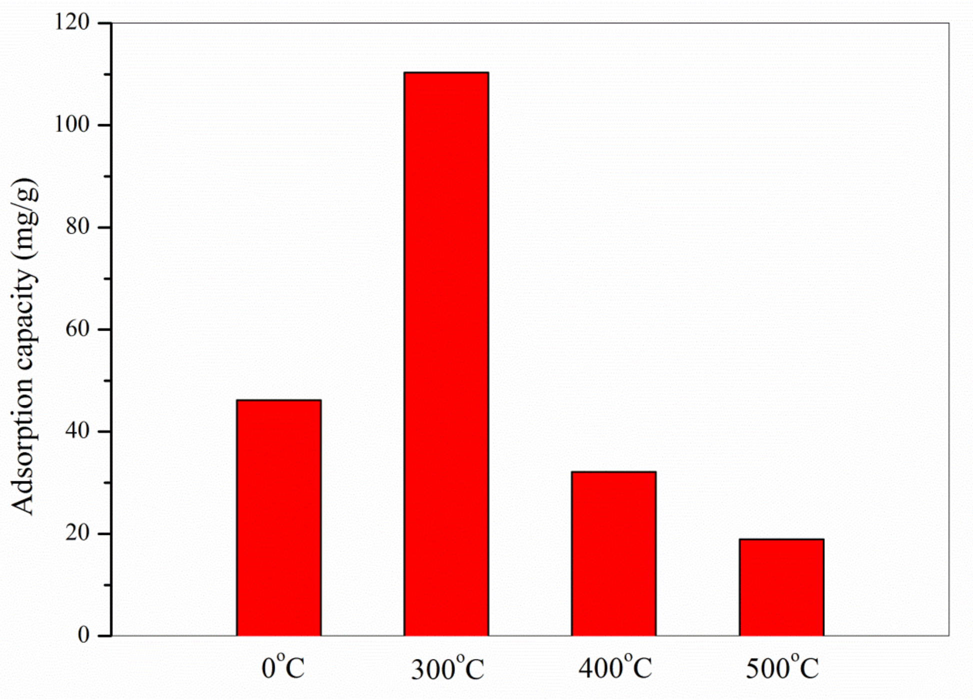

Fig. S7 Adsorption capacities of the precursor before and after calcination at 300 °C, 400 °C and 500 °C for fluoride

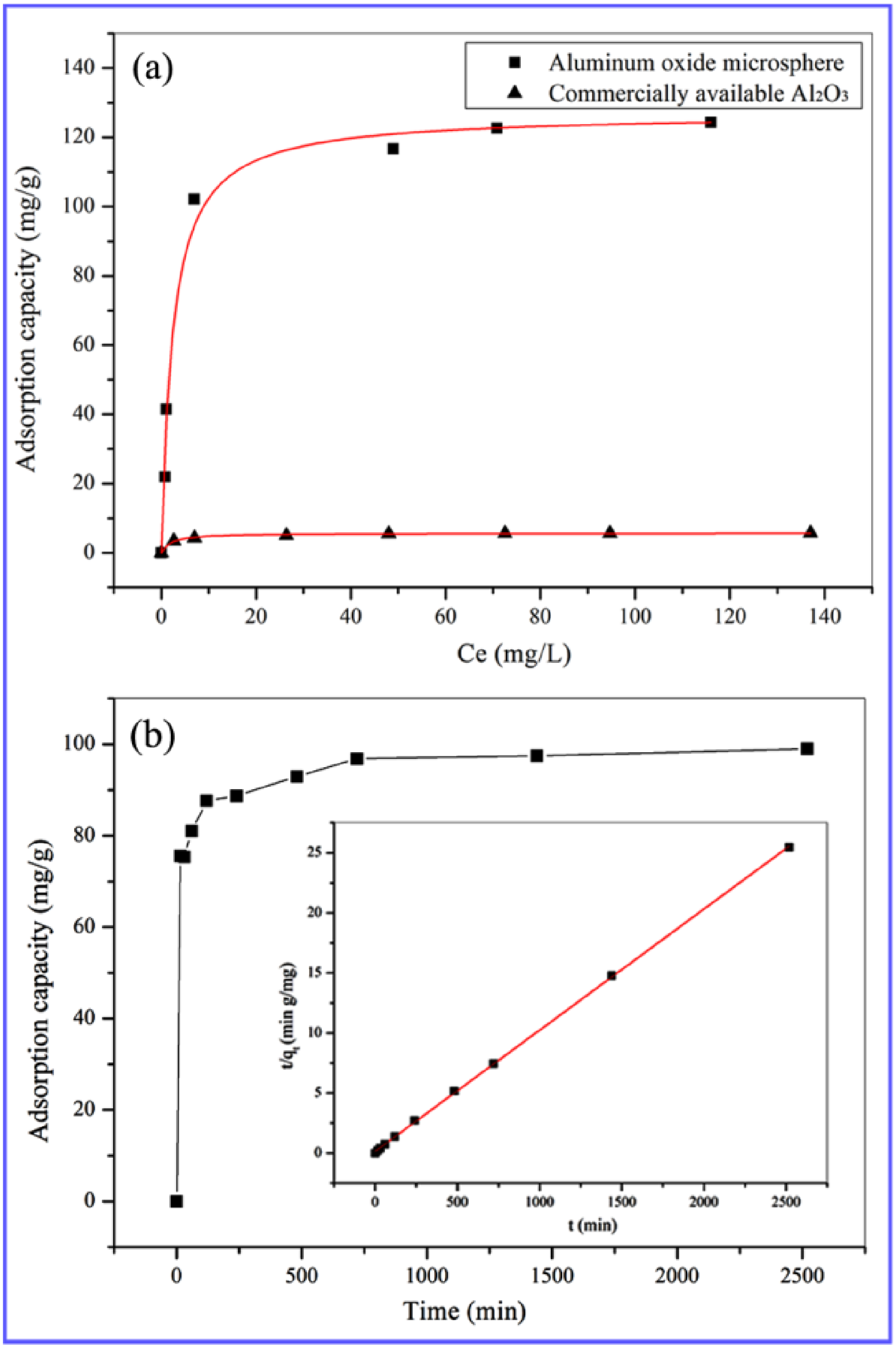

Fig. S8. (a) Adsorption isotherm; (b) adsorption kinetics and (inset) fitting curve of the pseudo-second-order model for fluoride removal using the final product.

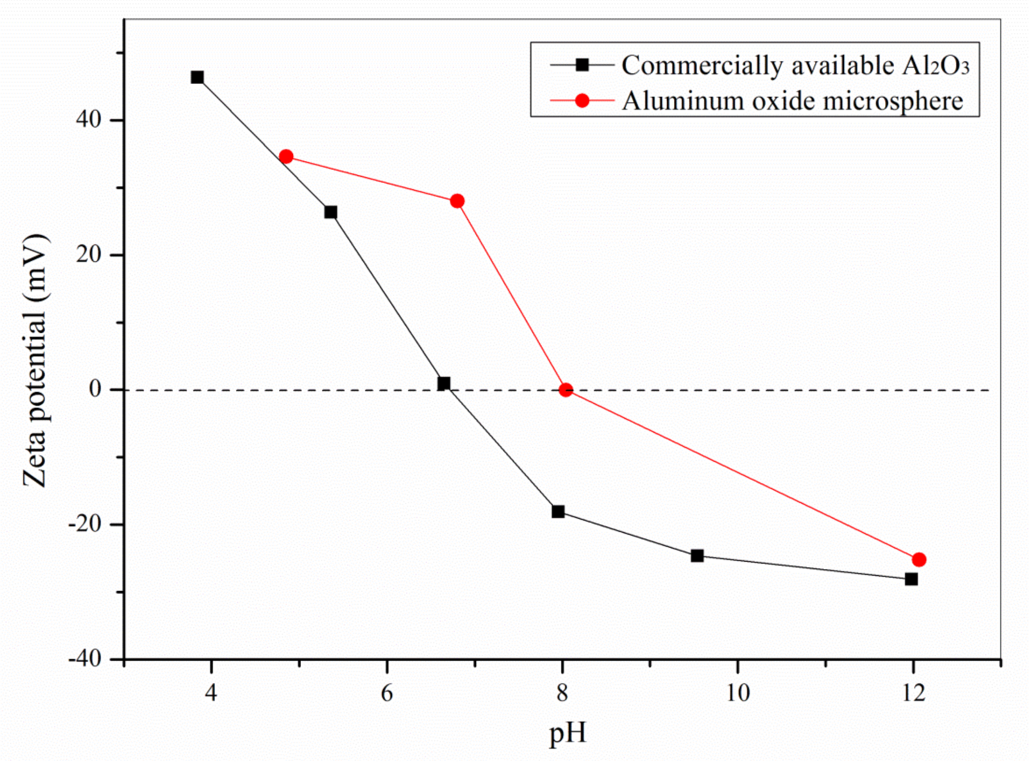

Fig. S9 IEPs of the final product and the commercially available Al_2O_3

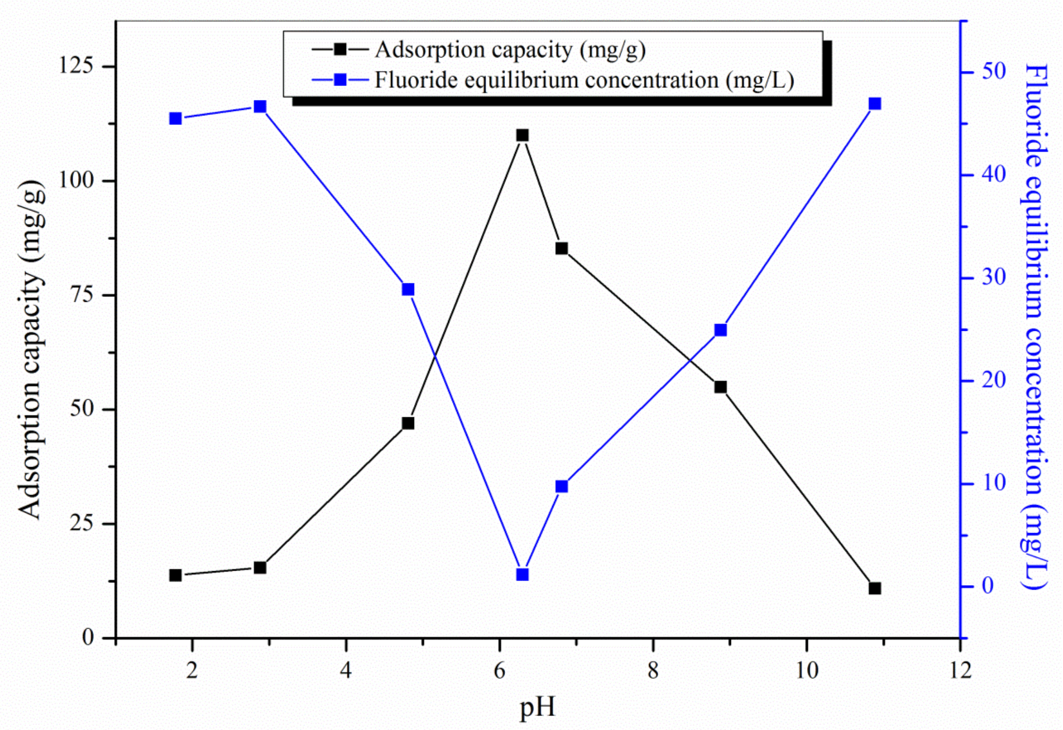

Fig. S10 Adsorption envelope for fluoride on the as-prepared material

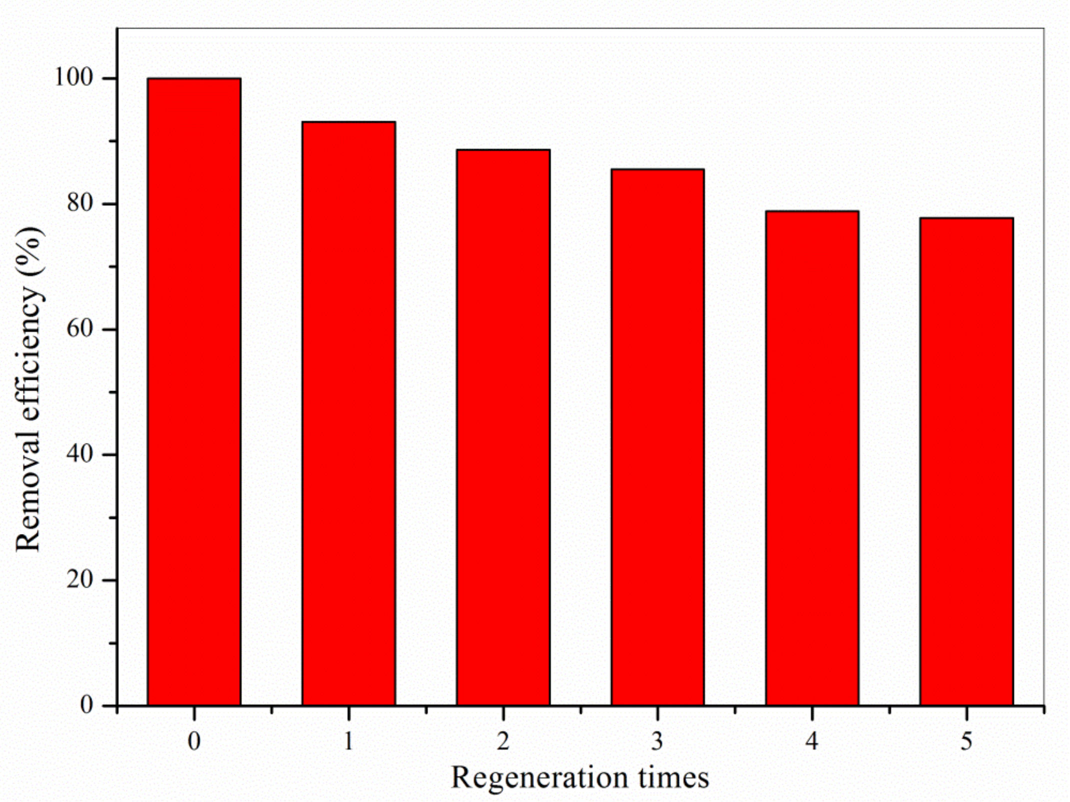

Fig. S11 Regeneration test for the final product

Table S1 BET surface areas of the as-prepared precursor calcined at different temperatures.

Calcination temperature (°C)	BET surface area (m^2/g)	Average pore diameter (nm)	Pore volume (cm^3/g)
0	62	2.769	0.101
300	376	1.410	0.664
400	182	7.452	0.474
500	148	8.529	0.429

Table S2 Langmuir adsorption model parameters for fluoride adsorption onto the as-prepared materials and commercially available Al_2O_3

Adsorbents	Langmuir adsorption model parameters		
	q_m (mg/g)	b (L/mg)	R^2
as-prepared materials	126.9	0.42	0.9865
commercially available Al_2O_3	5.7	0.52	0.9937

Table S3 Adsorption kinetic parameters obtained by Pseudo-second-order model

Pseudo-second-order model parameters			
$q_{e(theo)}$(mg/g)	k_2 (g mg^{-1}min^{-1}/10^{-4})	R^2	$q_{e(exp)}$(mg/g)
99.21	6.69	0.9998	98.9